Effect of ionic strength on shear-thinning nanoclay-polymer composite hydrogels

SCHOLARONE™
Manuscripts

Effect of ionic strength on shear-thinning nanoclay-polymer composite hydrogels

Amir Sheikhi[1,2,3,4+], Samson Afewerki[1,2,+], Rahmi Oklu[5], Akhilesh K. Gaharwar[6,7,8*], Ali Khademhosseini[1,2,3,4,9,10,11,12*]

[1]Biomaterials Innovation Research Center, Division of Biomedical Engineering, Department of Medicine, Brigham and Women's Hospital, Harvard Medical School, Cambridge, MA 02139, USA.

[2]Harvard-MIT Division of Health Sciences and Technology, Massachusetts Institute of Technology, Cambridge, MA 02139, USA.

[3]Department of Bioengineering, University of California - Los Angeles, 410 Westwood Plaza, Los Angeles, CA 90095, USA.

[4]Center for Minimally Invasive Therapeutics (C-MIT), California NanoSystems Institute (CNSI), University of California - Los Angeles, 570 Westwood Plaza, Los Angeles, CA 90095, USA.

[5]Division of Vascular & Interventional Radiology, Mayo Clinic, Scottsdale, Arizona 85259, USA.

[6]Department of Biomedical Engineering, Texas A&M University, College Station, TX 77843, USA.

[7]Department of Materials Science and Engineering, Texas A&M University, College Station, TX 77843, USA.

[8]Center for Remote Health Technologies and Systems, Texas A&M University, College Station, TX 77843, USA.

[+]These authors contributed equally to this work.

[*]Corresponding Author Email: gaharwar@tamu.edu (AKG); khademh@ucla.edu (AK)

[9]Department of Radiology, David Geffen School of Medicine, University of California - Los Angeles, 10833 Le Conte Ave, Los Angeles, CA 90095, USA.

[10]Department of Chemical and Biomolecular Engineering, University of California - Los Angeles, 5531 Boelter Hall, Los Angeles, CA 90095, USA.
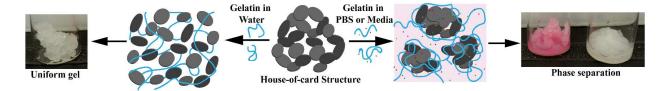
[11]Department of Bioindustrial Technologies, College of Animal Bioscience and Technology, Konkuk University, Seoul, 143-701, Republic of Korea.

[12]Center of Nanotechnology, Department of physics, King Abdulaziz University, Jeddah, 21569, Saudi Arabia.

Synopsis

The effect of ionic strength on the structure and rheological properties of nanoclay-gelatin shear-thinning biomaterials (STBs) is investigated. A fundamental insight into nanoclay-polymer interactions in physiological environments is provided to design clay-based biomaterials for biomedical applications.

TOC

Abstract

Nanoclay-polymer shear-thinning composites are designed for a broad range of biomedical applications, including tissue engineering, drug delivery, and additive biomanufacturing. Despite the advances in clay-polymer injectable nanocomposites, colloidal properties of layered silicates are not fully considered in evaluating the *in vitro* performance of shear-thinning biomaterials (STBs). Here, as a model system, we investigate the effect of ions on the rheological properties and injectability of nanoclay-protein hydrogels to understand their behavior when prepared in physiological media. In particular, we study the effect of sodium chloride (NaCl) and calcium chloride ($CaCl_2$), common salts in phosphate buffered saline (PBS) and cell culture media (e.g., Dulbecco's Modified Eagle's Medium, DMEM), on the structural organization of nanoclay (Laponite XLG-XR, a hydrous lithium magnesium sodium silicate)-polymer composites, responsible for the shear-thinning properties and injectability of STBs. We show that the formation of nanoclay-polymer aggregates due to the ion-induced shrinkage of diffuse double layer and eventually the liquid-solid phase separation decrease the resistance of STB against elastic deformation, decreasing the yield stress. Accordingly, the stress corresponding to the onset of structural breakdown (yield zone) is regulated by the ion type and concentration. These results are independent of the STB composition and can directly be translated into the physiological conditions: in the presence of salts, exfoliated nanoclay-based hydrogels undergo visually undetectable aggregation upon mixing with gelatin, resulting in heterogeneous hydrogels that phase separate under stress. This work provides fundamental insights into nanoclay-polymer interactions in physiological environments, paving the way for designing clay-based injectable biomaterials.

Introduction

Designing nanoengineered materials with unique physical and chemical properties for biomedicine,[1–3] tissue engineering and regenerative medicine,[4,5] drug delivery,[6–9] and translational medicine[10] relies on taking advantage of, often unprecedented, small-scale structural features. Newly-emerged biomaterials with nanoengineered rheological properties provide injectable platforms[11,12] for minimizing surgical complications while setting the stage for minimally-invasive procedures and, potentially, a variety of bench-to-bed-side translational applications, addressing unmet clinical challenges. As an example, we have recently developed an injectable shear thinning biomaterial (STB) for endovascular embolization[13] and hemorrhage treatment.[14] Despite the promising performance of STB as an embolic agent, little is known about the effect of physiological media during the fabrication process on the properties of these polymer nanocomposites.

The STB consists of Laponite XLG-XR (nanosized lithium magnesium sodium silicate) and gelatin (denatured collagen). Laponite is a two-dimensional (2D) disc-shaped nanoparticle with a thickness ~ 1 nm and diameter ~ 20–50 nm.[15,16] Properties, such as excellent biocompatibility, facile gel formation, high surface area (> 350 m^2 g^{-1}), and degradation into non-toxic products, i.e., sodium ions (Na^+), magnesium ions (Mg^{2+}), silicic acid (H_4SiO_4), and lithium ions (Li^+) have made Laponite an attractive candidate for biomedical applications,[17] including drug delivery,[18] tissue adhesives,[19] tissue engineering[20,21] and additive manufacturing.[22]

The surface of Laponite particles are negatively charged, while the edges bear positive charges, providing edge-rim electrostatic attraction, which results in a physical, reversible edge-rim binding. This unique feature allows Laponite dispersions to attain a shear-thinning behavior in which the colloidal network is temporarily destructed under an external shear, and upon the elimination of shear, it is reconstructed.[23] To date, understanding the structural dynamics and aging,[24–27] as well as the rheological properties of Laponite-based systems have been the focus of research.[26,28–33] Depending on the pH, H^+ or OH^- may dissociate from the nanoclay edge.[33] Dissociation of H^+ from the edge occurs beyond the point of zero charge pH (isoelectric point, pH ~ 11 for Mg-OH),[34] resulting in completely negatively charged particles. Below the isoelectric pH, the nanoclay releases OH^-, increasing pH. Moreover, Mg^{2+} on the Laponite may leach into the solution at pH<9, resulting in nanoparticle dissolution.[35,36]

When the exfoliated nanoclay is mixed with gelatin (partially hydrolyzed collagen, bearing positively and negatively charged moieties), a strong electrostatic attraction between the polymer and nanoparticles results in the formation of a physically crosslinked hydrogel.[37] The presence of ions in the solution may result in shielding the surface charge of Laponite nanoparticles, which impairs the self-assembly of nanodiscs into a "*house-of-cards*" structure. Additionally, the ratio between Laponite and polymer is important to prevent the formation of a coacervate solution wherein a colloid-rich phase is separated from the dispersion.[38] Despite the focus on the colloidal behavior of nanoclay in aqueous media, little effort is devoted to understand the key properties of polymer-nanoclay composite hydrogels prepared in the physiologically relevant media.

In this study, to shed light on the STB behavior in physiological media, we investigate the effect of common monovalent and divalent ions in PBS and cell culture media, namely NaCl and $CaCl_2$, on the structural and rheological properties of Laponite-gelatin shear-thinning biomaterials. We provide fundamental insights into the STB behavior when the fully exfoliated Laponite gel is mixed with gelatin in water, sodium chloride (NaCl), calcium chloride ($CaCl_2$), phosphate buffered saline (PBS), and cell culture medium (DMEM), resulting in distinct structural and physical properties. We will systematically show that ions, regardless of STB composition, result in heterogeneous gels, leading to phase separation upon applying a high shear. We anticipate that the fundamental aspects of gelatin-Laponite interactions in physiological media will lead to better understanding and fabrication of nanoclay-polymer shear-thinning biomaterials, suitable for a wide range of biomedical applications.

Materials and Methods

Materials

Laponite XLG-XR was purchased from BYK USA INC. Phosphate buffered saline (PBS) and Dulbecco's Modified Eagle Medium (DMEM) were provided by ThermoFisher Scientific. Gelatin Type A, 300 G, Bloom G1890, sodium chloride, and calcium chloride were supplied by Sigma Aldrich.

Methods

Sample preparation for rheology: To prepare Laponite 6%-gelatin 1% shear-thinning biomaterials, gelatin 0.1 g was transferred to a centrifuge tube (10 mL), containing 5 mL of a

desired medium (Milli-Q water, NaCl solution, $CaCl_2$ solution, PBS, or DMEM), followed by incubation at 37^oC until it fully dissolved. In parallel, Laponite (0.6 g) was added to a centrifuge tube (10 mL) containing cold Milli-Q water (5 mL, 4^oC), followed by immediate vortexing (~ 15 min) until a transparent gel was formed (self-regulated pH ~ 10, no buffer was used). Afterwards, 3.0 g gelatin (2 wt%) and 3.0 g nanoclay gel (12 wt%) were added to a falcon tube and immediately vortexed to solidify (~ 15 min). Subsequently, the material was incubated for 10 min at 37^oC and then cooled down to room temperature for 30 min prior measurements. Other STB compositions were prepared similarly.

Sample preparation for dynamic light scattering (DLS): Laponite with a desired concentration was added to cold Milli-Q water ($4°C$) and immediately vortexed until a transparent homogenous dispersion was obtained. In parallel, the gelatin with a desired concentration was added to the medium and incubated at 37^oC until fully dissolved. Subsequently, equal amounts of Laponite dispersions and gelatin solutions were mixed and vortexed for 1 minutes, prior measurements.

DLS analysis: The hydrodynamic size and ζ-potential of silicate nanoplatelets and the dispersions of silicate and gelatin were determined in ultrapure water (Milli-Q), PBS (pH = 7.4) and DMEM (pH = 7.4) using Zetasizer Nano series (Malvern Instruments). The samples were characterized immediately after preparation by placing them in a capillary cell (Disposable folded capillary cell DTS1070). All measurements were conducted at 25^oC in, at least, three replicates.

Oscillatory shear rheology: Rheological properties of STBs prepared in various media were characterized with an AR-G2 Rheometer (TA Instruments). Viscoelastic moduli were registered using a cone and plate geometry (20 mm or 40 mm diameter, 1° or 2° cone angle, respectively) with a truncation gap ~ 56 μm. Samples were loaded to the plate and allowed to equilibrate for 2 minutes. Oscillatory stress sweep was conducted at ~ 0.1-1000 Pa under an oscillatory frequency ~ 1 Hz, and oscillatory frequency sweep was performed at 0.1-100 Hz under an oscillatory stress ~ 10 Pa for all samples at 25°C or 37°C. The viscoelastic moduli versus shear stress and angular frequency were registered.
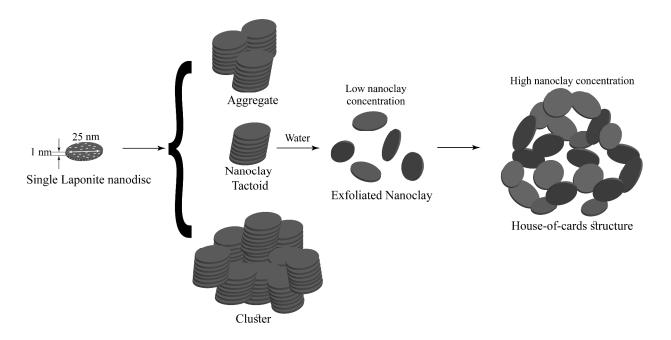
Injection force analysis: The injectability of the materials was analyzed using a mechanical tester (Instron Model 5542) equipped with a 100 N load cell, using a 3 mL Luer Lock syringe

with a 23 G needle (BD Precision Glide 23 G x 1 in Thin Wall M, with L = 38 mm, ID = 0.34 mm) or a catheter (5-French, length ~ 70 cm, 5F-Beacon Tip Torcon NB Advantage Catheter, Cook Medical). The Flow rate ~ 2 mL min^{-1} (injection rate ~ 33.96 mm min^{-1}).

Results and discussion

To understand the behavior of STB in physiological media, first, the rheological properties of its components, Laponite and gelatin, were studied. In the dry state, Laponite XLG-XR exists in microscale tactoids (10–100 μm, Na$^+$-mediated stacked layers of silicate) (**Scheme 1**).[39] The negative charge on Laponite surfaces is originated from the partial substitution of Mg^{2+} with Li$^+$ ions, and the positively-charged edges of Laponite predominantly contain magnesium hydroxide (MgOH).[40] When Laponite powder is dispersed in water, the tactoids are hydrated through Na$^+$ dissociation, rendering a permanent negative charge to the particle surfaces, resulting in the exfoliation of stacked structures into individual particles (**Scheme 1**).[39] The key mechanism regulating the exfoliation process of Laponite is Na$^+$ adsorption/desorption from the tactoids during hydration, which is affected by the addition of salts to the solutions, as well as pH variations. When Laponite nanodiscs are not fully exfoliated due to the presence of ions, they tend to form clusters of stacked discs with dimensions >100 nm (**Scheme 1**).[41]

The formation of stable gels depends on the solid concentration and incubation time. Dispersed Laponite ≥ 3 % w/v forms a physical gel within several minutes as a result of the self-assembly of exfoliated nanodiscs into a "*house-of-cards*" structure through face-to-edge attractions (**Scheme 1**).[42] We realized that Laponite (3 wt%) formed a gel after 16 h incubation in Milli-Q water at room temperature. At a lower nanoclay concentration (≤ 3% w/v), the process of gel formation is significantly slow. Earlier studies have reported that << 1 wt% Laponite may form a gel after several months.[43]

Scheme 1. *Schematic of a single Laponite disc, tactoids, aggregates, clusters, and possible structural evolution in an aqueous medium, namely exfoliation through which a stable gel may be obtained by forming a "house-of-cards" structure.*

Dynamics of self-assembly in Laponite-gelatin STBs

Figure 1 presents the ζ-potential and equivalent hydrodynamic size of colloidal particles in Laponite and Laponite-gelatin dispersions. Laponite attains a net negative charge (ζ-potential ~ -40 mV) upon dispersion in Milli-Q water, as a result of Na^+ dissociation (**Figure 1**). Despite the net negative charge of Laponite particles, increasing its concentration beyond 3 wt% results in the formation of colloidal gels, reflected in the hydrodynamic size increase from ~ 55 nm (fully exfoliated nanoplatelets) to ~ 400 nm (house-of-cards network) after only 4 h (**Figure 1a**). After mixing Laponite with a low concentration (0.01%) gelatin solution in water, the size and ζ-potential do not change significantly, possibly due to the low gelatin-to-Laponite ratio (e.g., 1:100) as well as the net negative charge of gelatin type A at the equilibrium pH (~ 10) of Laponite dispersions (**Figure 1a-d**). Importantly, the hydrodynamic size increased by increasing the gelatin content (e.g., 0.1%, **Figure 1c**) and Laponite concentration (2%, **Figure S1**). When [gelatin]/[Laponite] ~ 0.01, the hydrodynamic size of colloidal particles is similar to individual laponite particles, because gelatin is not able to induce colloidal aggregation. Increasing gelatin

concentration ([gelatin]/[Laponite] ~ 0.1) results in a 3-fold increase in the colloidal size, which may be attributed to the formation of intercalated Laponite-gelatin particles. Note that the hydrodynamic size does not change within 16 h, possibly due to the stability of colloidal clusters with ζ-potential ~ -40 mV. Addition of Laponite to gelatin solutions, prepared in PBS or the medium, increases the hydrodynamic size by several orders of magnitude, attesting to the formation of large aggregates (**Figure 1**). Images of Laponite, gelatin, and Laponite-gelatin biomaterials at various concentrations, prepared in different media are presented in **Figures S2 and S3**.
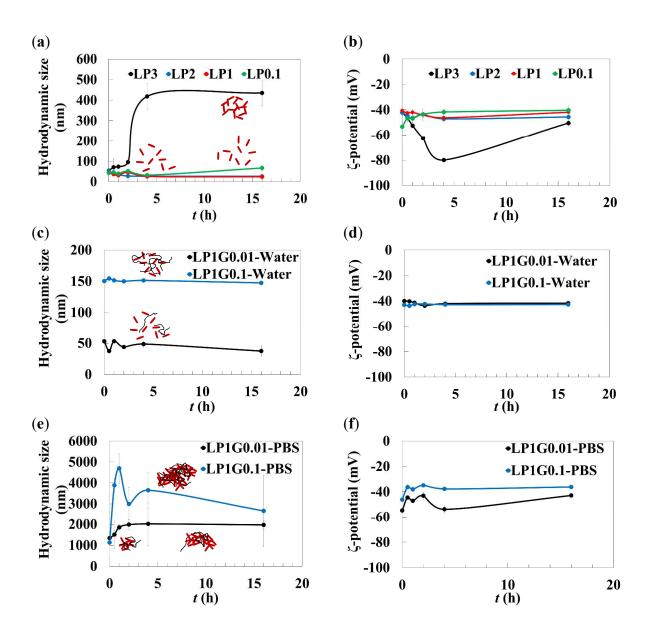
Figure 1. *Dynamic light scattering (DLS) and electrokinetic analyses of Laponite (LP) dispersions and Laponite-gelatin (LP-G) nanocomposites: hydrodynamic size (**a**) and ζ-potential (**b**) of Laponite, hydrodynamic size (**c,e**) and ζ-potential (**d,f**) of Laponite-gelatin nanocomposites prepared in water or PBS. Schemes in the inset of panel **a** show the dynamics of Laponite-Laponite interactions. Schemes in the inset of panels **c** and **e** show the formation of intercalated/exfoliated (in water, **c**) or aggregated/tactoid-like (in PBS, **e**) Laponite-polymer nanocomposites.*

Rheological properties of Laponite and gelatin

Fully exfoliated Laponite results in the formation of a transparent colloidal gel. **Figure 2** presents the rheological properties of Laponite dispersions/gels, including the viscoelastic moduli versus angular frequency at room temperature. Note that we use the term "gel", instead of "glass", for Laponite dispersions with storage modulus G' > loss modulus G''. At room temperature, a low Laponite concentration (2 wt%) results in a weak gel with $G'' \sim G'$ within a wide range of angular frequency ($\omega \sim 0.1$–1000 rad s^{-1}). Increasing the Laponite concentration to 3 wt% and 6 wt% increases the storage and loss moduli by more than 2 and 3 orders of magnitude, respectively. Loss moduli decrease by increasing the oscillatory frequency for Laponite gels (3% and 6%), attesting to a decreasing trend of dynamic viscosity ($\eta' = G''/\omega$), a typical behavior of a shear-thinning material (besides the reduction of shear viscosity versus shear rate), originating from reversible electrostatic Laponite-Laponite binding. By increasing the temperature to 37°C, storage and loss moduli of Laponite gels (3 and 6 wt%) slightly increase, showing an enhanced network formation (**Figure S4, Supporting Information**), which is in agreement with the literature.[44,45] Similarly, gelatin, a heat-sensitive biopolymer has concentration- and temperature- dependent rheological properties. At room temperature (**Figure 2**), when the frequency increases from 1 to 100 Hz (100 times), the loss modulus G'' of gelatin solutions (3 wt%) increases ~ 10 times, showing that dynamic viscosity decreases by increasing ω. Increasing temperature to the physiological level (**Figure S5, Supporting Information**), storage and loss moduli decrease ~ 100 times, because gelatin, a thermosensitive biopolymer, undergoes gel-to-sol transition.

Laponite, *T*=25°C

(a)

(b)

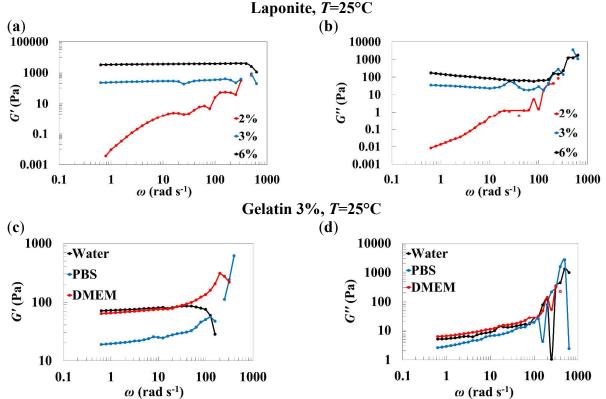**Gelatin 3%, *T*=25°C**

(c)

(d)

Figure 2. *Rheological properties of the shear-thinning biomaterial (STB) components, obtained from frequency sweeps. Storage (**a**) and loss (**b**) moduli of Laponite dispersions/gels, prepared in Milli-Q water. Increasing Laponite concentration increases the viscoelastic moduli. Storage (**c**) and loss (**d**) moduli of gelatin solutions at T = 25°C, prepared in Milli-Q water, PBS, and DMEM.*

Effect of monovalent and divalent ions on Laponite-gelatin STBs

Among the constituents of physiological media, sodium chloride (NaCl) and calcium chloride (CaCl$_2$) hold the highest concentrations. PBS, mimicking the osmolarity, ion concentration, and pH of body fluids comprises 137 mM NaCl, which is more than 90% of its total ion concentration. Cell culture media, such as DMEM (Dulbecco's Modified Eagle's Medium), one of the most common media, contain ~110 mM NaCl and 1.8 mM CaCl$_2$. Accordingly, NaCl and CaCl$_2$ may be considered as representative monovalent and divalent ion sources in physiological media, respectively. Note that other dominant sources of monovalent and divalent ions in PBS

and DMEM are potassium chloride KCl (2.7 mM in PBS and 5.3 mM in DMEM), sodium bicarbonate $NaHCO_3$ (~ 44 mM in DMEM), disodium phosphate Na_2HPO_4 (10 mM in PBS), and magnesium sulfate $MgSO_4$ (~0.8 mM in DMEM). Here, we study the effect of NaCl and $CaCl_2$ concentrations on the rheological properties of STB, made up of Laponite and gelatin.

Figures 3a-c present the storage and loss moduli versus oscillatory stress of STBs (6% Laponite-1% gelatin) prepared in Milli-Q water and 100 mM or 1000 mM of sodium chloride. In Milli-Q water ([NaCl] = 0 mM), the STB remains in the linear viscoelastic region (LVR) up to stress ~ 160 Pa. In this region, the material deformation (strain) is linearly correlated to the oscillatory shear. When the stress exceeds 160 Pa, the viscoelastic moduli start to decrease, as a result of the structural breakdown of STBs. In this region, material deformation is significant compared to the LVR, and the material starts to yield, meaning that it loses its structural integrity. The stress associated with the onset of structural breakdown may be considered as the yield stress.[46] The region between the yield point until reaching the fluid-like behavior ($G' < G''$) is called the yield zone. When STB is prepared in the NaCl solutions, the onset of structural breakdown shifts to a lower stress, meaning that the material becomes more susceptible to stress. The higher the NaCl concentration, the easier the STB undergoes structural breakdown; therefore, the yield zone occurs under a low stress.

Figure 3d compares the storage modulus of STBs versus oscillatory stress. When STB is prepared by mixing the exfoliated Laponite in Milli-Q water with gelatin in NaCl solutions, the storage moduli increases by increasing NaCl concentration up to 1000 mM. This may be attributed to the formation of intercalated Laponite-gelatin aggregates; however, the susceptibility of STB to stress increases. The increase in the viscoelastic moduli due to the aggregate formation has been reported in the literature for other colloidal systems, such as nanocellulose dispersions.[47] Up to ~ 10 mM NaCl, the storage modulus of STB does not significantly change when the stress increases from 1 to ~160 Pa, showing that the hydrogel may tolerate a high stress while holding its structural integrity. We call this STB a high-quality material for minimally-invasive procedures (e.g., injection), because it does not undergo irreversible phase separation when it is exposed to a high stress, for example during centrifugation (**Figure 3e**). When the ionic strength increases beyond 100 mM, the storage modulus starts decreasing at a relatively lower stress, and in an extreme case such as

centrifugation, the biphasic water-Laponite/gelatin, a liquid-solid coacervate, is formed (**Figure 3e**). Coacervates may hold promise for a range of applications; however, we call this STB a low-quality STB, because it undergoes phase separation and loses its reversible shear-thinning properties under a high stress.

The storage moduli of STBs, prepared at various NaCl concentrations, versus oscillatory frequency under an oscillatory stress ~ 10 Pa are presented in **Figure 3f**. Increasing the monovalent salt concentration increases the storage modulus. At such a low stress, STB resists the oscillatory frequency within 0.1 to 100 Hz, meaning that *G'* does not decrease; however, when it is injected through a needle (23 G, **Figure 3g**), heterogeneities become evident from the injection forces. In the absence of NaCl, STB may be injected smoothly with no significant fluctuations in the injection force plateau; whereas, even at a low NaCl concentration (e.g., 10 mM), severe fluctuations in the injection force are observed. Note that such heterogeneities may not be detected through typical oscillatory rheology.

Monovalent ions, such as Na^+, are able to screen the diffuse double layer of Laponite particles, which in turn decrease the long-range intra-particle (face-face) electrostatic repulsion, resulting in the formation of aggregates, mediate by the van der Waals attraction force. For colloidal particles dispersed in a solution of monovalent ions (1-1 electrolyte), the diffuse double layer thickness δ is proportional to the reciprocal square root of ion concentration ($\delta = (\varepsilon k_B T / (e^2 \Sigma z_i^2 n_i))^{1/2}$), where ε is the solvent permittivity, k_B is Boltzmann's constant, *T* denotes the absolute temperature, *e* is the proton charge, and z_i and n_i denote the ion charge and bulk concentration, respectively.[48] At 10 mM NaCl, δ ~ 3 nm, which decreases to ~ 0.3 nm at 1000 mM. Divalent ions, such as calcium ions (Ca^{2+}), besides a more significant charge screening effect (e.g., δ ~ 1.9 nm and 0.6 nm at 10 mM and 100 mM, respectively), may act as bridging ions, connecting two Laponites to each other from their negatively-charged faces. The bridging effect of Ca^{2+} results in the formation of aggregates at relatively lower concentrations than a monovalent ion, such as Na^+. Such an effect has been reported for several colloidal and polymeric systems, such as nanocelluloses.[49] The storage modulus of STB, prepared at different Ca^{2+} concentrations, versus oscillatory stress is presented in **Figure 3h**. At low ion concentrations ($\leq$10 mM), the storage modulus increases, similar to the STB behavior with Na^+. The increase in *G'*, however, is noticeably higher when STB is prepared in Ca^{2+} instead of Na^+.

When the Ca^{2+} concentration increases to 100 mM, G' significantly decreases, possibly as a result of phase separation during STB preparation (e.g., vortexing). The effect of salts on the yield stress is presented in **Figure 3i**. The yield stress decreases by increasing the salt concentration, regardless of the type of salt. Interestingly, the reduction in the yield stress is more significant when divalent ions are present during STB preparation. For example, at only 10 mM salt, the yield stress of STB does not change with Na^+, whereas, Ca^{2+} decreases it by ~ 600%. This may be explained by the bridging effect of divalent ions on the colloidal stability of Laponite particles.

Effect of PBS and cell culture medium (DMEM) on Laponite-gelatin STBs

To prepare cell-laden STBs, exfoliated Laponite gels are typically required to be added to a gelatin solution containing cells, which must, inevitably, comprise PBS or a cell culture medium. In the absence of ions, the electrostatic attraction of Laponite surface (bearing negative charges) and the rim (bearing positive charges) with the positively- (primary amines, $-NH_2$) and negatively- (carboxylic acid, -COOH) charged functional groups of gelatin, respectively, promotes physical, reversible crosslinking, forming shear-thinning hydrogels with concentration dependent properties. **Figure 4** presents the rheological properties of Laponite (6%)-gelatin (1%) hydrogels at room temperature, prepared by mixing fully exfoliated Laponite in Milli-Q water with gelatin solutions in Milli-Q water, PBS, or DMEM. When hydrogels are prepared in Milli-Q water, the storage and loss moduli (**Figure 4**) are significantly lower than hydrogels prepared in PBS or DMEM. For example, the Laponite (6%)-gelatin (1%) hydrogel prepared in PBS and DMEM at room temperature has a storage modulus in the order of 10 kPa and a loss modulus in the order of 1 kPa, respectively; whereas, $G' \sim$ order of 1 kPa and $G'' \sim$ order of 0.1 kPa in Milli-Q water (**Figure 4,** $\omega \sim$ 10 rad s^{-1}). This is in accordance with the effect of monovalent and divalent ions on the STB. Separation of the liquid phase from the STB when it is prepared in PBS or DMEM (**Figure 4c**) upon exposure to a high stress (e.g., centrifugation or injection) results in the formation of solid-rich coacervates. The phase separation is a result of ion-induced aggregation of intercalated Laponite-gelatin particles, yielding a heterogeneous hydrogel compared to the uniform gel obtained in the absence of ions. Note that all the frequency sweep experiments are conducted within the linear viscoelasticity region of the STBs.

We also investigate the effect of ions on the various compositions of STB. **Figure 5** presents the storage and loss moduli of STBs prepared in Milli-Q water, PBS, and DMEM, involving various laponite/gelatin ratios. When the concentration of Laponite ~ 2 % and gelatin ~ 1%, the STB is liquid-like ($G' \sim G''$), and upon the addition of PBS or DMEM, the precipitation of solid phase results in a decrease in storage and loss moduli. Increasing Laponite and gelatin concentrations results in $G' > G''$ in which case STB behavior in PBS and DMEM follows a similar trend as in the presence of monovalent and divalent ions: compared to Milli-Q water, the storage and loss moduli of STBs are higher when they are prepared in the presence of the ions (**Figure 5**). This may be a result of aggregate formation due to the high content of ions in the gelatin solutions prepared in PBS and the cell culture medium. Note that at a low oscillatory stress (~ 10 Pa) the shear-thinning behavior is maintained.

In the absence of ions, in all formulations, when [Laponite]/[gelatin] > 1, the viscoelastic moduli of the nanocomposite gels increase with increasing Laponite or gelatin concentrations (**Figure 5**). Interestingly, in PBS and DMEM, increasing the gelatin content of nanocomposites increases the storage and loss moduli regardless of Laponite concentration. When [Laponite]/[gelatin] ~ 1 (**Figure 5**), the nanocomposites form weaker gels (lower storage modulus) than [Laponite]/[gelatin] > 1. The loss moduli follow a similar trend wherein a higher solid content results in a higher G''. This behavior may be attributed to the inhibition of polymer-nanoclay interactions as a result of gelatin-mediated steric stabilization of Laponite. Excessive gelatin adsorbs on the Laponite surface, providing an excluded volume around the nanodiscs, weakening the nanocomposites due to the impaired electrostatic attraction. It has previously been reported that the optimum binding of gelatin-Laponite occurs at the ratio ~ 0.36.[50]

Note that, at low Laponite concentrations ($\leq$ 2 wt%, **Figures S6** and **S7**), the viscoelastic properties of the nanocomposites are dominated by gelatin. For example, storage and loss moduli of Laponite (2 wt%)-gelatin (3 wt%) are similar to those of gelatin (**Figure S5**). However, by increasing the Laponite concentration, the contribution of nanodiscs to the viscoelasticity of hydrogels becomes more pronounced (**Figure 5**). With increasing the gelatin content (**Figure 5**), an increase in the storage (G') and loss moduli (G'') of the hydrogels was observed for a wide range of angular frequency (0.1–1000 rad s[-1]). For example, at Laponite concentration ~ 6%, with an increase in gelatin content from 1 wt% to 3 wt%, a significant increase in G', from 4.6 to

17.2 kPa, and in *G''*, from 0.2 to 2.7 kPa were observed (**Figure 5)**. Accordingly, besides the ionic strength, the viscoelastic properties of nanocomposites, prepared in any media, are directly affected by the ratio of Laponite to gelatin.
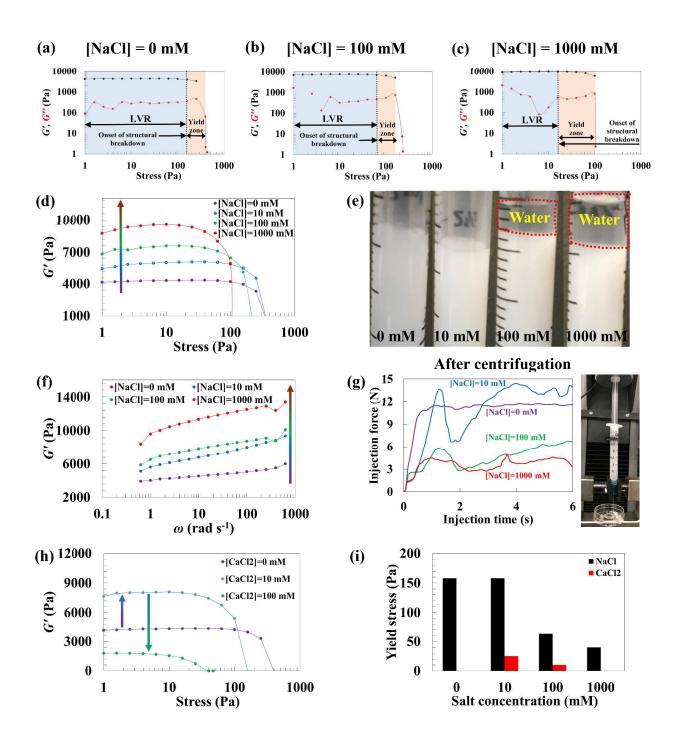
Figure 3. *Effect of monovalent and divalent ions on the rheological properties of STB (Laponite 6%, gelatin 1%). Effect of sodium chloride concentration on the storage and loss moduli of STB at [NaCl] = 0 mM (**a**), 100 mM (**b**), and 1000 mM (**c**), showing that the higher the Na$^+$ concentration, the lower stress is required for the STB to undergo structural breakdown and, eventually, yield. Comparison of storage moduli G' versus oscillatory stress for STBs prepared in Milli-Q water, and in 10-1000 mM NaCl (**d**). Images of STBs prepared at different concentrations of NaCl after centrifugation at 3000 rpm for 1 min. Coacervate formation is evident at [NaCl]≥100 mM (**e**). Storage modulus G' versus oscillatory frequency for STBs prepared in Milli-Q water, and 10-1000 mM NaCl (**f**). Injection force of STBs through a 23 G needle, using a 3 mL syringe (**g**). Heterogeneity of STB is reflected in the force fluctuations at [NaCl]≥10 mM. Storage modulus G' versus oscillatory stress for STBs prepared in Milli-Q water, and 0-100 mM CaCl$_2$ (**h**). Yield stress versus NaCl and CaCl$_2$ concentrations (**i**).*

Laponite 6%-Gelatin 1%, *T*=25°C

(a)

(b)

(c)

Uniform gel   Gelatin in Water   House-of-card Structure   Gelatin in PBS or Media   Phase separation
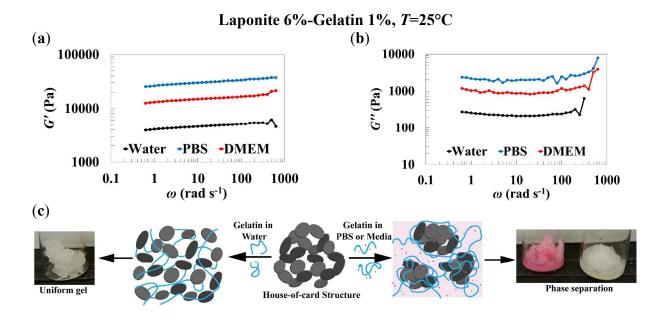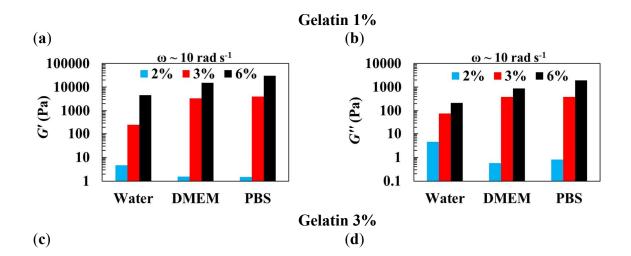
Figure 4. *Viscoelastic moduli of Laponite (6%)-gelatin (1%) shear-thinning hydrogels prepared by mixing exfoliated Laponite with gelatin dissolved in Milli-Q water, PBS, and cell culture medium (DMEM) at 25°C. Storage (**a**) and loss moduli (**b**) versus angular frequency. When STB is prepared in Milli-Q water, a uniform gel is yielded; whereas, STB prepared in PBS or DMEM undergoes phase separation under a high stress, e.g., centrifugation or injection (**c**).*
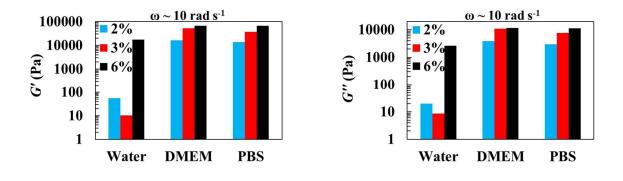
Gelatin 1%

(a)

(b)

Gelatin 3%

(c)

(d)

Figure 5. *Effect of Laponite concentration on the rheological properties of Laponite-gelatin shear-thinning hydrogels prepared by mixing exfoliated Laponite with gelatin (1%, **a,b**, and 3%, **c,d**) dissolved in Milli-Q water, PBS, and cell culture medium (DMEM) at 25°C. Storage moduli (**a,c**), and loss moduli (**b,d**) at ω ~ 10 rad s^{-1} show that when G'>G'', STBs prepared in PBS or DMEM attain a higher viscoelastic moduli than those prepared in Milli-Q water, possibly due to the formation of, often visually unrecognizable, micro-scale Laponite-gelatin aggregates. These STBs readily phase separate under a high stress, e.g., upon injection through needles or standard catheters for minimally-invasive procedures, increasing the risk of blockage and consequent health complications. Note that when G' < G'', adding ions to the STBs, decrease the viscoelasticity as a result of solid precipitation.*
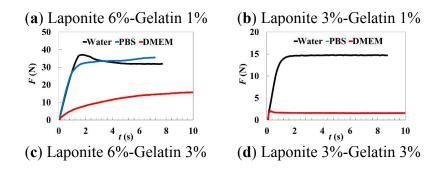
As discussed earlier, a facile method to investigate the homogeneity of STBs is to measure their injectability through needles or catheters, an essential property for minimally invasive applications. Heterogeneity may result in stress-mediated phase separation, leading to complications such as blockade during medical procedures. The injection force of the STBs prepared in different media were measured using a clinical catheter (5F, Shepherd Hook, SOFT-Vu). The shear-thinning property of nanocomposites results in an initial resistance against the shear, reflected in an increase in the injection force, followed by a plateau. The injection force for Laponite (6%, **Figure S8**) *F* ~ 10.9 N, which decreases by decreasing nanoparticle concentration (e.g., *F* ~ 4.5 N for 3% Laponite). **Figure 6** presents the injection force of various STB compositions (Laponite ~ 3% and 6%, gelatin ~ 1% and 3%), prepared in Milli-Q water, PBS, and DMEM. The injection force for the Laponite-gelatin nanocomposites, prepared in

water, displays a similar trend to the viscoelastic moduli (e.g., **Figure 5)**: composites with a higher solid content require higher injection forces.

The homogeneity of nanocomposites results in a smooth injection force plateau (**Figure 6**, hydrogels prepared in water); whereas, the heterogenous structure of nanocomposites prepared in high ionic strengths is reflected in severe force fluctuations (**Figure 6**). In an extreme case, the phase separation results in a large injection force plateau for the compact nanocomposites, or an extremely low injection force due to the drainage of solvent. Note that Laponite 6%-gelatin 3% gels prepared in PBS or DMEM were not injectable through the catheter, where a blockage occurred immediately as a result of heterogeneity and large aggregate formation. For the biomaterials prepared in PBS, only Laponite 6%-gelatin 1% showed an optimal injection force ($F \sim$ 34.4 N, **Figure 6**). However, even though the injection force of Laponite 6%-gelatin 1% prepared in PBS displays a smooth trend, corresponding to a macroscopically homogenous material, the heterogeneous nature of the composite was revealed by injecting it through a 23 G needle (**Figure 3**). The heterogeneity of Laponite 3%-gelatin 3% prepared in PBS is evident in the injection force plateau fluctuations in **Figure 6**.

Movies S1 and **S2** show the injection of STBs, prepared in water, PBS, or DMEM, through a needle. A smooth and easily-injectable material was obtained when water was the only solvent; however, for the materials prepared in PBS or DMEM, first, a liquid phase exists the needle after which the solid-like material is injected, confirming the coacervate formation, heterogeneity, and phase separation of the nanoclay-based hydrogels (See also *Figure S2*).

(a) Laponite 6%-Gelatin 1% **(b)** Laponite 3%-Gelatin 1%
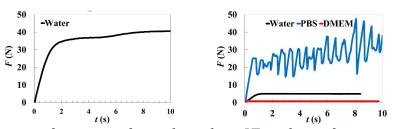**(c)** Laponite 6%-Gelatin 3% **(d)** Laponite 3%-Gelatin 3%

Figure 6. Dynamics of injection force through a 5F catheter for various compositions of Laponite-gelatin shear-thinning hydrogels prepared in different media. The shear-thinning properties of hydrogels results in an increase in force upon injection, reaching a plateau. When the hydrogels are prepared in water, the plateau is smooth, attesting to the material homogeneity; whereas, hydrogels prepared in PBS or DMEM undergo phase separation, resulting in fluctuations in the injection force plateau due to heterogeneity. Note that in case of phase separation, extremely high or low injection forces as a result of aggregate formation or solvent drainage may be observed. Note that in panel c, the hydrogels prepared in PBS or DMEM were not injectable.

Conclusions

Nanoclay-polymer nanocomposites are promising biomaterials for a broad range of biomedical applications, such as tissue engineering and therapeutic delivery. Colloidal aspects of nanoclays (Laponite), bearing a heterogeneous charge distribution, impart unique rheological properties to nanoclay-based shear-thinning biomaterials (STB), wherein a polyampholyte macromolecule, e.g., gelatin, forms a reversible shear-responsive network. To understand the properties of STBs prepared in physiological media, we systematically investigated the viscoelastic properties of Laponite-gelatin nanocomposite hydrogels prepared in NaCl, $CaCl_2$, PBS, and a cell culture medium (DMEM). Despite the apparent increase in the storage and loss moduli of STBs, prepared in the presence of monovalent and divalent ions, the formation of, often visually unnoticeable, nanoclay-polymer clusters, strongly deteriorate the recovery of network under stress, decreasing the resistance against elastic deformation and the yield stress. Ion-mediated coacervate formation and phase separation of STBs under shear result in impaired injectability, which may endanger patients' lives, particularly during minimally-invasive procedures. This work sheds light on the role of media in regulating complex interactions between the nanoclay and polymers for developing homogeneous shear-thinning biomaterials, providing fundamental

understanding of nanoclay-polymer interactions, which may pave the way for designing and preparing robust STBs.

Acknowledgments

References

(1)   Bhat, S.; Kumar, A. Biomaterials and Bioengineering Tomorrow's Healthcare. *Biomatter* **2013**, *3*, e24717(1)-e24717(12).

(2)   Khademhosseini, A.; Peppas, N. A. Micro-and Nanoengineering of Biomaterials for Healthcare Applications. *Adv. Healthc. Mater.* **2013**, *2*, 10–12.

(3)   Tibbitt, M. W.; Rodell, C. B.; Burdick, J. A.; Anseth, K. S. Progress in Material Design for Biomedical Applications. *PNAS* **2015**, *112*, 14444–14451.

(4)   Kerativitayanan, P.; Tatullo, M.; Khariton, M.; Joshi, P.; Perniconi, B.; Gaharwar, A. K. Nanoengineered Osteoinductive and Elastomeric Scaffolds for Bone Tissue Engineering. *ACS Biomater. Sci. Eng.* **2017**, *3*, 590–600.

(5)   Mousa, M.; Evans, N. D.; Oreffo, R. O. C.; Dawson, J. I. Clay Nanoparticles for Regenerative Medicine and Biomaterial Design: A Review of Clay Bioactivity. *Biomaterials* **2018**, *159*, 204–214.

(6)   Rwei, A. Y.; Wang, W.; Kohane, D. S. Photoresponsive Nanoparticles for Drug Delivery. *Nano Today* **2015**, *10*, 451–467.

(7)   Kalhapure, R. S.; Suleman, N.; Mocktar, C.; Seedat, N.; Govender, T. Nanoengineered Drug Delivery Systems for Enhancing Antibiotic Therapy. *J. Pharm. Sci.* **2015**, *104*, 872–905.

(8)   Sukhorukov, G. B.; Rogach, A. L.; Zebli, B.; Liedl, T.; Skirtach, A. G.; Köhler, K.; Antipov, A. A.; Gaponik, N.; Susha, A. S.; Winterhalter, M. Nanoengineered Polymer Capsules: Tools for Detection, Controlled Delivery, and Site-Specific Manipulation. *Small* **2005**, *1*, 194–200.

(9)   Sun, T.; Zhang, Y. S.; Pang, B.; Hyun, D. C.; Yang, M.; Xia, Y. Engineered Nanoparticles for Drug Delivery in Cancer Therapy. *Angew. Chemie Int. Ed.* **2014**, *53*, 12320–12364.

(10)   Cai, W. *Engineering in Translational Medicine*; Springer, 2014.

(11)   Zhang, Z. Injectable Biomaterials for Stem Cell Delivery and Tissue Regeneration. *Expert Opin. Biol. Ther.* **2017**, *17*, 49–62.

(12)   Vernon, B. *Injectable Biomaterials: Science and Applications*; Elsevier, 2011.

(13)   Avery, R. K.; Albadawi, H.; Akbari, M.; Zhang, Y. S.; Duggan, M. J.; Sahani, D. V; Olsen, B. D.; Khademhosseini, A.; Oklu, R. An Injectable Shear-Thinning Biomaterial for Endovascular Embolization. *Sci. Transl. Med.* **2016**, *8*, 365ra156-365ra156.

(14)   Gaharwar, A. K.; Avery, R. K.; Assmann, A.; Paul, A.; McKinley, G. H.; Khademhosseini, A.; Olsen, B. D. Shear-Thinning Nanocomposite Hydrogels for the Treatment of Hemorrhage. *ACS Nano* **2014**, *8*, 9833–9842.

(15)   Ruzicka, B.; Zaccarelli, E.; Zulian, L.; Angelini, R.; Sztucki, M.; Moussaïd, A.; Narayanan, T.; Sciortino, F. Observation of Empty Liquids and Equilibrium Gels in a Colloidal Clay. *Nat. Mater.* **2011**, *10*, 56–60.

(16)   Carrow, J. K.; Cross, L. M.; Reese, R. W.; Jaiswal, M. K.; Gregory, C. A.; Kaunas, R.; Singh, I.; Gaharwar, A. K. Widespread Changes in Transcriptome Profile of Human Mesenchymal Stem Cells Induced by Two-Dimensional Nanosilicates. *Proc. Natl. Acad. Sci.* **2018**, *115*, E3905–E3913.

(17)   Tomás, H.; Alves, C. S.; Rodrigues, J. Laponite®: A Key Nanoplatform for Biomedical Applications? *Nanomedicine Nanotechnology, Biol. Med.* **2017**.

(18)   Wang, S.; Wu, Y.; Guo, R.; Huang, Y.; Wen, S.; Shen, M.; Wang, J.; Shi, X. Laponite Nanodisks as an Efficient Platform for Doxorubicin Delivery to Cancer Cells. *Langmuir* **2013**, *29*, 5030–5036.

(19)   Liu, Y.; Meng, H.; Konst, S.; Sarmiento, R.; Rajachar, R.; Lee, B. P. Injectable Dopamine-Modified Poly (Ethylene Glycol) Nanocomposite Hydrogel with Enhanced Adhesive Property and Bioactivity. *ACS Appl. Mater. Interfaces* **2014**, *6*, 16982–16992.

(20)   Gaharwar, A. K.; Mihaila, S. M.; Swami, A.; Patel, A.; Sant, S.; Reis, R. L.; Marques, A. P.; Gomes, M. E.; Khademhosseini, A. Bioactive Silicate Nanoplatelets for Osteogenic Differentiation of

Human Mesenchymal Stem Cells. *Adv. Mater.* **2013**, *25*, 3329–3336.

(21)   Chang, C.-W.; van Spreeuwel, A.; Zhang, C.; Varghese, S. PEG/Clay Nanocomposite Hydrogel: A Mechanically Robust Tissue Engineering Scaffold. *Soft Matter* **2010**, *6*, 5157–5164.

(22)   Wilson, S. A.; Cross, L. M.; Peak, C. W.; Gaharwar, A. K. Shear-Thinning and Thermo-Reversible Nanoengineered Inks for 3D Bioprinting. *ACS Appl. Mater. Interfaces* **2017**, *9*, 43449–43458.

(23)   Cummins, H. Z. Liquid, Glass, Gel: The Phases of Colloidal Laponite. *J. Non. Cryst. Solids* **2007**, *353*, 3891–3905.

(24)   Bellour, M.; Knaebel, A.; Harden, J. L.; Lequeux, F.; Munch, J.-P. Aging Processes and Scale Dependence in Soft Glassy Colloidal Suspensions. *Phys. Rev. E* **2003**, *67*, 31405(1)-31405(8).

(25)   Saha, D.; Joshi, Y. M.; Bandyopadhyay, R. Investigation of the Dynamical Slowing down Process in Soft Glassy Colloidal Suspensions: Comparisons with Supercooled Liquids. *Soft Matter* **2014**, *10*, 3292–3300.

(26)   Joshi, Y. M.; Reddy, G. R. K.; Kulkarni, A. L.; Kumar, N.; Chhabra, R. P. Rheological Behaviour of Aqueous Suspensions of Laponite: New Insights into the Ageing Phenomena. In *Proceedings of the Royal Society of London A: mathematical, physical and engineering sciences*; The Royal Society, 2008; Vol. 464, pp. 469–489.

(27)   Bonn, D.; Tanase, S.; Abou, B.; Tanaka, H.; Meunier, J. Laponite: Aging and Shear Rejuvenation of a Colloidal Glass. *Phys. Rev. Lett.* **2002**, *89*, 15701(1)-15701(4).

(28)   Lapasin, R.; Abrami, M.; Grassi, M.; Šebenik, U. Rheology of Laponite-Scleroglucan Hydrogels. *Carbohydr. Polym.* **2017**, *168*, 290–300.

(29)   Li, H.; Ren, W.; Zhu, J.; Xu, S.; Wang, J. Rheology and Processing of Laponite/Polymer Nanocomposites. *Rheol. Process. Polym. Nanocomposites* **2016**, 383–404.

(30)   Pek-Ing, A.; Yee-Kwong, L. Surface Chemistry and Rheology of Laponite Dispersions—Zeta Potential, Yield Stress, Ageing, Fractal Dimension and Pyrophosphate. *Appl. Clay Sci.* **2015**, *107*, 36–45.

(31)   Boucenna, I.; Royon, L.; Guedeau-Boudeville, M.-A.; Mourchid, A. Rheology and Calorimetry of Microtextured Colloidal Polycrystals with Embedded Laponite Nanoparticles. *J. Rheol. (N. Y. N. Y).* **2017**, *61*, 883–892.

(32)   Dávila, J. L.; d'Ávila, M. A. Laponite as a Rheology Modifier of Alginate Solutions: Physical Gelation and Aging Evolution. *Carbohydr. Polym.* **2017**, *157*, 1–8.

(33)   Valencia, G. A.; Moraes, I. C. F.; Hilliou, L. H. G.; Lourenço, R. V.; do Amaral Sobral, P. J. Nanocomposite-Forming Solutions Based on Cassava Starch and Laponite: Viscoelastic and Rheological Characterization. *J. Food Eng.* **2015**, *166*, 174–181.

(34)   Martin, C.; Pignon, F.; Piau, J.-M.; Magnin, A.; Lindner, P.; Cabane, B. Dissociation of Thixotropic Clay Gels. *Phys. Rev. E* **2002**, *66*, 21401(1)-21401(11).

(35)   Thompson, D. W.; Butterworth, J. T. The Nature of Laponite and Its Aqueous Dispersions. *J. Colloid Interface Sci.* **1992**, *151*, 236–243.

(36)   Mourchid, A.; Levitz, P. Long-Term Gelation of Laponite Aqueous Dispersions. *Phys. Rev. E* **1998**, *57*, R4887–R4890.

(37)   Li, C.; Mu, C.; Lin, W.; Ngai, T. Gelatin Effects on the Physicochemical and Hemocompatible Properties of Gelatin/PAAm/Laponite Nanocomposite Hydrogels. *ACS Appl. Mater. Interfaces* **2015**, *7*, 18732–18741.

(38)   Karimi, F.; Qazvini, N. T.; Namivandi-Zangeneh, R. Fish Gelatin/Laponite Biohybrid Elastic Coacervates: A Complexation Kinetics–structure Relationship Study. *Int. J. Biol. Macromol.* **2013**, *61*, 102–113.

(39)   Dawson, J. I.; Oreffo, R. O. C. Clay: New Opportunities for Tissue Regeneration and Biomaterial Design. *Adv. Mater.* **2013**, *25*, 4069–4086.

(40)   Laponite Technical Bulletin: Laponite: Structure, Chemistry and Relationship to Natural Clays.

1990, *L104–90–A*, 1–15.

(41)   Bippus, L.; Jaber, M.; Lebeau, B. Laponite and Hybrid Surfactant/Laponite Particles Processed as Spheres by Spray-Drying. *New J. Chem.* **2009**, *33*, 1116–1126.

(42)   Ruzicka, B.; Zaccarelli, E. A Fresh Look at the Laponite Phase Diagram. *Soft Matter* **2011**, *7*, 1268–1286.

(43)   Ruzicka, B.; Zulian, L.; Ruocco, G. Routes to Gelation in a Clay Suspension. *Phys. Rev. Lett.* **2004**, *93*, 258301(1)-258301(4).

(44)   Ramsay, J. D. F. Colloidal Properties of Synthetic Hectorite Clay Dispersions: I. Rheology. *J. Colloid Interface Sci.* **1986**, *109*, 441–447.

(45)   Ovarlez, G.; Coussot, P. Physical Age of Soft-Jammed Systems. *Phys. Rev. E* **2007**, *76*, 11406.

(46)   Shih, W. Y.; Shih, W.; Aksay, I. A. Elastic and Yield Behavior of Strongly Flocculated Colloids. *J. Am. Ceram. Soc.* **1999**, *82*, 616–624.

(47)   Lenfant, G.; Heuzey, M. C.; van de Ven, T. G. M.; Carreau, P. J. A Comparative Study of ECNC and CNC Suspensions: Effect of Salt on Rheological Properties. *Rheol Acta* **2017**, *56*, 51–62.

(48)   Verwey, E. J. W.; Overbeek, J. T. G. *Theory of the Stability of Lyophobic Colloids*; Dover: New York, 1948.

(49)   Sheikhi, A.; Safari, S.; Yang, H.; van de Ven, T. G. M. Copper Removal Using Electrosterically Stabilized Nanocrystalline Cellulose. *ACS Appl. Mater. Interfaces.* **2015**, *7*, 11301–11308.

(50)   Pawar, N.; Bohidar, H. B. Surface Selective Binding of Nanoclay Particles to Polyampholyte Protein Chains. *J. Chem. Phys.* **2009**, *131*, 07B617(1)-07B617(10).